

# Super multi-view 3-D display system based on focused light Array using reflective vibrating scanner array(ViSA)

□ Ho-In Jeon\* · Nak-Hee Jung\* · Jin-San Choi\* · Young Jung\* · Young Huh\*\* · Jung Sam Kim\*\*\*

\* Department of Electronic Engineering, Kyung-Won University, Korea [hijeon@mail.kyungwon.ac.kr](mailto:hijeon@mail.kyungwon.ac.kr)  
\*\* Korea Electrotechnology Research Institute, Chang-Won-Si, Korea  
\*\*\* Ministry of Information and Communication, Korean Government, Korea

## ABSTRACT

In this paper, we present a primitive system design of a super multi-view(SMV) 3-D display system based on a focused light array(FLA) concept using reflective vibrating scanner array(ViSA). The parallel beam scanning using a vibrating scanner array is performed by moving left and right an array of curvature-compensated mirrors or diamond-ruled reflective grating attached to a vibrating membrane. The parallel laser beam scanner array can replace the polygon mirror scanner which has been used in the SMV 3-D display system based on the focused light array(FLA) concept proposed by Kajiki at TAO(Telecommunications Advancement Organization). The proposed system has great advantages in the sense that it requires neither huge imaging optics nor mechanical scanning parts. Some mathematical analyses and fundamental limitations of the proposed system are presented. The proposed vibrating scanner array, after some modifications and refinements, may replace polygon mirror-based scanners in the near future.

*Keywords: 3-D display system, Super multi-view, Focused light array, Vibrating scanner array, Reflection grating, Polygon mirror, Galvanometer, Diamond ruled reflective grating*

## 1. INTRODUCTION

While most information is communicated through 2-D images or printed words, most data channels transfer only a series of data elements. Therefore, to manipulate the information for either transmission or reception, a 2-D image space must be transformed to or from a single function of time. This is what scanners do, and we can say that, in our information age, scanning is as fundamental to information transfer as vision is to perception. Scanners can serve to both input and output information.

There are several types of optical scanners. The most widely used scanner is a galvanometer scanner, due to its easy configuration and cheap price. Polygon mirror scanners that are used in laser printers also provide very good scanning quality. Bar code readers harness the holographic scanning method. Acousto-optic and electro-optic scanners are often used in systems that require accurate scanning quality. Optical disk scanners are used in storage systems such as CD-ROMs. Aside from the applications that are mentioned here, scanning systems also play very important roles in implementing 3-D display systems.

3-D display systems (See [1], [2], [3], [4] and references therein.) can be implemented in

various ways. The fundamental mechanisms for the implementation of 3-D display system can be classified into three categories: spatial multiplexing; temporal multiplexing; and angular multiplexing. 3-D display systems utilizing optical plates such as lenticular screen, parallax barrier, and holographic screens that are used to generate viewing zones belong to the spatial multiplexing scheme. Field-sequential binocular stereoscopic videos with polarizing glasses or LCD shutters are of the temporal-multiplexing type. The 3-D display system based on FLA(Focused Light Array) may be classified as the angular multiplexing category.

3-D display systems that utilize spatial-multiplexing scheme suffer from the resolution limitations of the display devices as the number of images to be presented increases. An electroholographic 3D display system that utilizes a polygon mirror and galvanometer scanner [5], stationary polygon mirror incorporated with 6 AOMs(Acousto-Optic Modulator) [6], or 5 LCDs with optical combiners [7], records and displays the data based on a spatial multiplexing, and thus suffers from the resolution limitation problem of the display devices. On the other hand, 3-D systems based on the temporal-multiplexing scheme have to solve the speed limitations of electronics and refreshing speed of CRT or LCD projectors if one wants to increase the

number of images for the purpose of alleviating the unnaturalness of discrete parallaxes and providing better viewing zones. Multi-view 3D display systems with CRT projectors and holographic screens [8] are utilizing basically temporal multiplexing, and thus speed of electronics and switches are limiting factors. Even though spatio-temporal multiplexing [9] can increase the number of images that can be presented to user's eyes by a factor of 2, there exists a fundamental limitation that we cannot increase the number of images dramatically without any special breakthrough technologies.

The concept of Focused Light Array (FLA) proposed by Kajiki [10] can solve these

problems, as shown in Fig. 1, by presenting simultaneously as many images as one wants, superimposed but separated by less than the pupil size of the viewer. This is called the Super Multi-view(SMV) region. An implementation of the FLA using a galvanometer and a polygon mirror scanner has been demonstrated by TAO with the simultaneous scanning of the 45 images. However, polygon mirrors and galvanometers have their own disadvantages in that the scanning requires mechanical rotation which is delicate with respect to external physical impact. More than that, the system requires that the imaging optics should be as large as the size of the screen and viewing angle. These problems can be solved by using an array of curvature-compensated parallel laser beam scanning method that has been recently presented in [11].

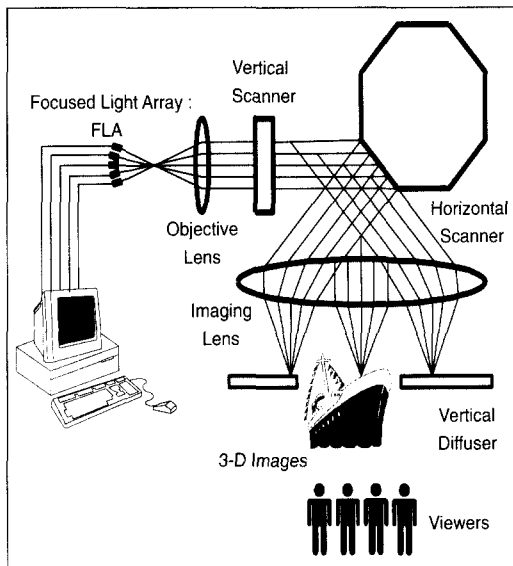


Figure 1. Super Multi-View 3-D display system based on FLA(Focused Light Array) concept using polygon mirror and galvanometer scanner.

the operating principles of the proposed system is given in Sec. 3. Section 4 demonstrates a specific design example of the super multi-view 3-D display system using the vibrating curvature-compensated mirror scanner array. Another specific design example of super multi-view 3-D display system using diamond-ruled reflective grating scanner array is presented in Sec. 5. Finally, conclusions are given in Sec. 6.

## 2. CHARACTERIZATION OF GALVANOMETER AND POLYGON MIRROR SCANNERS

Galvanometer scanners are used extensively in laser scanning systems. From an optical point of view, they have several advantages. The scanning mirror can rotate about an axis in the plane of mirror. The mirror can then be located at the entrance pupil of the lens system and its position does not move as the mirror rotates. Moreover, the  $F-\theta$  condition is often not required, because the shaft angular velocity of the mirror can be controlled electronically to provide uniform spot velocity. Finally, galvanometer systems are suitable for XY scanning. The principal disadvantage of galvanometer scanners is that they are limited in writing velocity. Galvanometer scanners provide the easiest way to design an XY scanner. The two mirrors, however, have to be

separated from each other, and this means that the optical system has to work with two separated entrance pupils, with considerable distance between them. This, in effect, requires that the lens system be aberration-corrected for a much larger aperture than the laser beam diameter. A system demanding large aperture and field then will have different degrees of distortion correction for the two directions of scan.

Polygon and holographic scanners are mainly used for applications that require severe uniformity of scanning velocity, sometimes as low as 0.1%, with addressability of a few microns, and high-speed scanning velocities. In the design of lens systems for polygons, some optical effects must be considered. These include: bow; beam displacement; and cross scan error.

The incoming and exiting beams must be located in a single plane which is perpendicular to the polygon rotation axis. Errors in achieving this condition will displace the spot in the cross-scan direction by an amount which varies with the field angle. This results in a curved scan line, called bow. The spot displacement  $E$  as a function of field angle is given by the equation

$$E = F \sin \alpha \left[ \frac{1}{\cos \theta} - 1 \right], \quad (1)$$

where  $F$  is the focal length of the lens,  $\theta$  is the field angle, and  $\alpha$  is the angle between the incoming beam and the plane that is perpendicular to the rotation axis.

The optical axis of the focusing lens should be coincident with the center of the input laser beam, referred to as the feed beam. Any error will introduce bow. The bow introduced by the input beam not being in the plane perpendicular to the rotation can, however, be compensated for, to some extent, by tilting the lens axis. A second peculiarity of the polygon is that the facet rotation occurs around the polygon center rather than the facet face. This causes a facet displacement of the collimated beam as the polygon rotates. This displacement of the incoming beam means that the lens must be well corrected over a large aperture than the laser beam diameter.

The polygons usually have pyramidal errors in the facets as well as some axis wobble. These cause cross-scan errors in the scan line. These errors must be small, for the eye is extremely sensitive in spotting them. Some printing systems are achieving more than 1000 dots/inch performance. This means that the maximum cross-scan error in this case should be much less than  $25 \mu\text{m}$ . A system with no cross-scan error correction using a 700 mm focal length lens, would require pyramid error no larger than 2 arc seconds. Three ways to correct for the

cross-scan error in polygons are (1) the use of cylindrical lens, (2) anamorphic beam on the facet, and (3) the retroflective prism.

### 3. OPERATING PRINCIPLES OF THE PROPOSED SYSTEM

To explain the operating principles of the proposed system, we refer to Fig. 2. The video signals modulate the laser diode array and the multiple light rays are incident on the corresponding curvature-compensated mirrors of the mirror array. By moving the mirror array left and right, all the light rays are reflected in a parallel manner to hit the diffuser screen simultaneously. Each of the laser diode beams is scanned at the same time by using curvature-compensated mirror array as shown in the circle of Fig. 2. The reflecting mirror

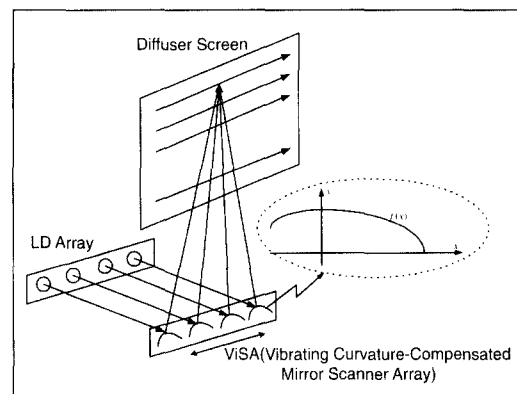


Figure 2. Super Multi-View 3-D display system based on parallel laser beam scanning using curvature-compensated mirror scanner array.

compensates the scanning speed at the screen to guarantee uniform intensity of the scanned light.

Fig. 3 shows one mirror element, shown in the circle of Fig. 2, through which we can determine the shape function. This function also describes the mode of the laser beam reflection and scanning mechanism. We let the curve of the mirror attached to a sinusoidally vibrating actuator moving in the +x and -x axis be a function  $f(x)$  that is to be determined. The distance between the screen and the reflecting mirror is set to be  $D$ .

The center of the mirror is assumed to be located at  $x = 0$ , and the height  $r$  is  $r = f(0)$ . At time  $t = 0$ , the laser beam is incident on the point  $O$ , and we want the beam to be reflected back through exactly the same path as it gets in. This requires that  $f'(0) = 0$ . After  $t$  seconds,

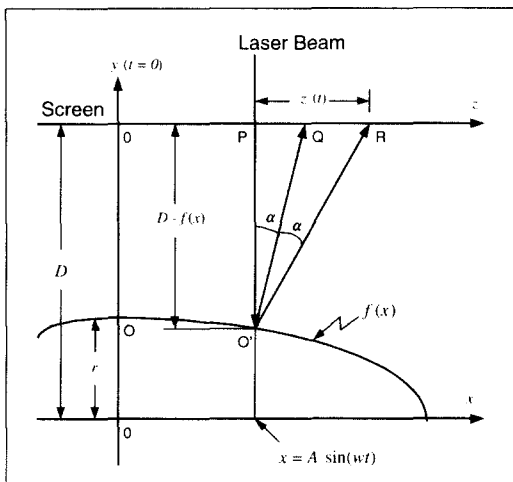


Figure 3. One mirror element of the parallel beam scanner with curvature compensated.

the mirror moves to the left by the amount  $x = A \sin(\omega t)$ , where  $A$  is the maximum deviation of the mirror that can move from the origin, and the laser beam hits the point  $S$ . Then the beam is reflected to hit the screen at the position  $R$  according to the reflection law, where  $\alpha$  is the angle between the vertical line and the normal line at the point  $S$ . From a simple geometric analysis and reflection law, we can get the position  $z(x)$  of the reflected beam at the screen as

$$z(x) = [D - f(x)] \tan 2\alpha = 2[D - f(x)] \frac{f'(x)}{[f'(x)]^2 - 1} \quad (2)$$

Now, the point  $z(x)$  that the reflected light hits over the screen needs to move at a certain constant speed such that the intensity is uniform everywhere over the scanning line of the screen. Therefore, the function  $z(x)$  has to be evaluated at  $x = A \sin(\omega t)$  to produce

$$z(t) = \left[ \frac{2\{D - f(A \sin \omega t)\} f'(A \sin \omega t)}{[f'(A \sin \omega t)]^2 - [w A \cos(\omega t)]^2} \right] w A \cos(\omega t) \quad (3)$$

and the uniform intensity is guaranteed if the derivative of the function  $z(t)$  with respect to  $t$  is set to be a constant  $C$ . Our goal is to find the function  $f(x)$  by solving the differential equation  $z'(t) = C$ , where  $t$  is evaluated at  $t = \sin^{-1}(x/A)/\omega$ . Even though it is not impossible to find the derivative of the function  $z(t)$ , it is

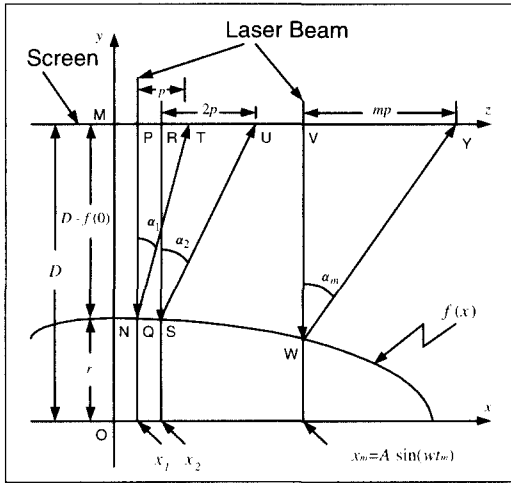


Figure 4. Linearization of the nonlinear problem

a tedious and space-wasting job to write the result in this paper. What we can easily guess, though, is that the differential equation is highly nonlinear. Runge-Kuta method did not work for our case. To obtain a reasonable result  $f(x)$  for the curvature-compensated mirror, we simplify the nonlinear problem to have a linear differential equation. The result of the linearization process for the nonlinear differential equation to analyze the curvature-compensated mirror scanner is shown in Fig. 4.

As shown in Fig. 4, the laser beam hits the point N at time  $t = 0$  and is reflected back to hit the point M which is the path that it enters. At  $t = t_1$ , the point  $x_1$  moves to point O, and the beam will hit the point Q. At this point we want the reflected beam to hit the point T

which is separated by  $p$  from the point P, where  $p$  is the resolution of the screen that users can determine for their specific applications. The relationship between  $p$  and  $\alpha_1$  can be written as

$$[D - f(x_1)] \tan \alpha_1 = p. \quad (4)$$

At  $t = t_2$ , the point  $x_2$  moves to point O, and the beam hits the point S and is reflected to hit the point U. For uniform speed of scanning, we want the distance between R and U to be  $2p$ , to give the relation

$$[D - f(x_2)] \tan \alpha_2 = 2p. \quad (5)$$

Generalizing this procedure at  $t = t_m$ , we can see that the point  $x_m$  moves to point O, and the reflected beam hits the point W and is reflected to hit the point Y which is separated by  $mp$  from the point V. This can be written as

$$[D - f(x_m)] \tan \alpha_m = mp, \quad (6)$$

where

$$\tan(\alpha_m) = \frac{-2f'(x_m)}{1 - [f'(x_m)]^2}. \quad (7)$$

Rewriting Eq. (6) and (7), we obtain

$$mp[1 - \{f'(x_m)\}^2] = -2f'(x_m)[D - f(x_m)]. \quad (8)$$

As we have expected already, this is a nonlinear differential equation. If we assume, however, that the function  $f(x)$  does not change too much in the

vibrating range compared with the distance  $D$ , then we can write  $D - f(x_m)$  as a constant  $D - r$ , and we can simplify this nonlinear equation to a linear equation by solving the following quadratic equation given by

$$mp[f'(x_m)]^2 - 2[D - r]f'(x_m) - mp = 0 \quad (9)$$

Recall that the movement of the membrane is symmetric. Therefore, it is sufficient to consider only right hand side of mirror, and the sign of the slope  $f'(x_m)$  should be negative to give

$$f'(x_m) = \frac{(D - r) - \sqrt{(D - r)^2 + m^2 p^2}}{mp} \quad (10)$$

Finally, we can find the linear equation  $f_m(x)$  at the point  $x_m$  as

$$f_m(x) = A_m x + B_m \quad (11)$$

where  $A_m$  can be obtained from Eq. (10) with  $A_0 = 0$ , and  $B_m$  will be determined iteratively from the initial condition of the curvature-compensated mirror, that is,  $B_0 = r = f_0(0)$ , and

$$f_m\left(\frac{x_m + x_{m-1}}{2}\right) = f_{m-1}\left(\frac{x_m + x_{m-1}}{2}\right) \quad (12)$$

From Eqs. (10), (11), and (12), we can design our curvature-compensated mirror scanner as well as the screen size. In Sec. 4, we will show some computation results for the scanning systems.

#### 4. AN EXAMPLE OF SCANNER SYSTEM DESIGN AND COMPUTATION RESULTS

As a design example of the curvature-compensated mirror, we have selected the screen that can be used as a practical 3-D display terminal. In other words, the size of the screen has been chosen to be 400 mm x 300 mm. Since we want the terminal to be able to support the VGA mode (640 x 480), the resolution of the screen then becomes  $p = 400/640 = 0.625$  mm. The distance between the CCMS and the screen has been set to be  $D = 100$  mm.

Based on these parameters and equations given in Eq. (10) to (12), the computer computations for three different cases of the remaining parameters with (1)  $A = 10$ ,  $r = 1$ , (2)  $A = 1$ ,  $r = 0.3$ , and (3)  $A = 4$ ,  $r = 1$  have been performed to find the curvature function  $f(x)$ , and the results are shown in Figs. 5, 6, and 7, respectively. From these figures, we can see

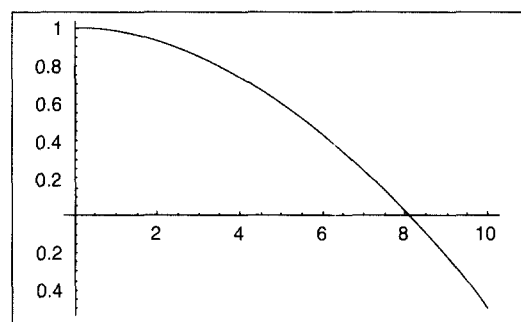
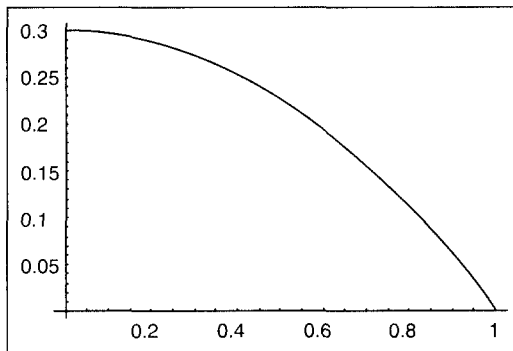
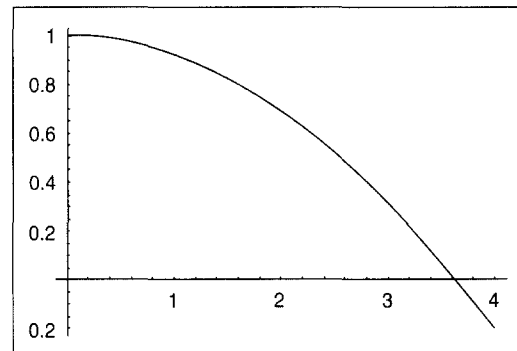


Figure 5. The shape function  $f(x)$  with  $A = 10$ ,  $r = 1$



Figure 6. The shape function  $f(x)$  with  $A = 1$ ,  $r = 0.3$ Figure 7. The shape function  $f(x)$  with  $A = 4$ ,  $r = 1$ 

that they are just scaled down for each case. The ratio of the depth of the mirror to the maximum deviation was always 3. This means that we can design CCMS as small as we want, depending upon the types of the vibrating membranes. The beam width of the laser will be the only factors that will affect the performance of the system when we make the mirror element of the scanner array very small.

### 5. 3-D DISPLAY SYSTEM WITH REFLECTIVE GRATING SCANNER ARRAY

The new super multi-view 3-D display system using curvature-compensated vibrating mirror scanner array can reduce, to some extent, the drawbacks of the Kajiki system. Even though it is not impossible to design a super multi-view 3-D display system using curvature-compensated mirror scanner array as

explained in previous sections, it is extremely difficult to complete the system because it requires a very precise construction of an array of curvature-compensated mirrors. We can avoid these difficulties if we replace the curvature-compensated mirror elements, as shown in Fig. 2, by diamond-ruled diffraction gratings.

In this section, we characterized diffraction gratings that can be used for super multi-view 3-D display systems as a scanning element, and then proposed a way of utilizing this concept by specifying and computing the design parameters that has to be determined. The diffraction gratings have been extensively investigated in Richardson Grating Laboratory, where they manufacture all kinds of gratings. For reader's convenience and referral purposes of explaining the proposed system, we briefly review some characteristics of gratings. We recommend readers to read the "Diffraction Grating Handbook" written by Christopher

Palmer at Richardson Grating Laboratory [12, 13] and references therein.

Diffraction grating is an optical element that separates incident polychromatic radiation into its constituent wavelength. A diffraction grating disperses incident light. This occurs when electromagnetic radiation contacts an obstruction with dimensions similar to wavelength of the impinging radiation. When the obstruction is periodic, as is the case with gratings, radiation is dispersed as a function of the angle of incidence, its wavelength and the spacing between the periodic obstructions.

A reflection grating consists of a series of equally spaced parallel grooves formed in a reflective coating deposited on a suitable substrate. On the other hand, the transmission grating consists of a grating superimposed on a transparent optical surface. The distance between adjacent grooves and the angle the groove form with respect to the substrate influence both the dispersion and efficiency of a grating. If the wavelength of the incident radiation is much larger than the groove spacing, diffraction will not occur. On the other hand, if the wavelength is much smaller than the groove spacings, the facets of the groove will act as a mirror and, again, no diffraction will take place.

The way in which the grooves are formed separates gratings into two basic types:

holographic and ruled. Physically forming grooves into a reflective surface with a diamond mounted on a ruling engine produces ruled gratings. Gratings produced from laser-constructed interference patterns and a photolithographic process are known as interference or holographic gratings.

Diffraction by a reflection grating can be visualized from the geometry in Fig. 8, which shows a light ray of wavelength  $\lambda$  incident at an angle  $\alpha$  and diffracted by a grating of groove spacing  $d$  along angles  $\beta_m$ . These angles are measured from the grating normal, which is the dashed line perpendicular to the grating surface at its center. The sign convention for these angles depends on whether the light is diffracted on the same side or the opposite side of the grating as the incident light. In Fig. 8, the angles  $\alpha > 0$  and  $\beta_1 > 0$ , since they are measured counter-clockwise from the grating normal, while the angles  $\beta_0 < 0$  and  $\beta_{-1} < 0$ ,

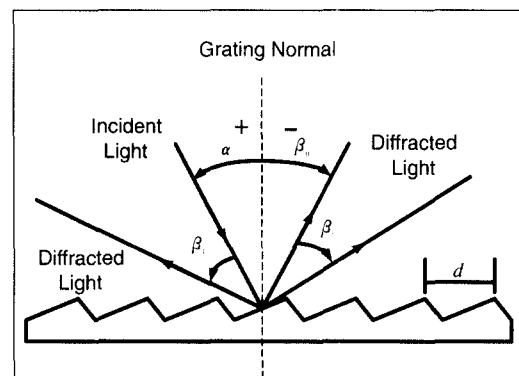


Figure 8. Reflection Grating

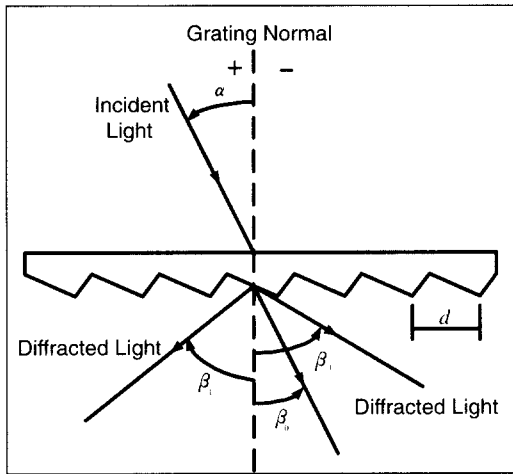


Figure 9. Transmission Grating

since they are measured from clockwise from the grating normal. Figure 9 shows a transmission grating. By convention, angles of incidence and diffraction are measured from the grating normal to the beam. This is shown by arrows in the figures. In both figures, the sign convention for angles is shown by the plus and minus symbols located on either side of the grating normal. For either reflection or transmission gratings, the algebraic signs of two angles differ if they are measured from opposite sides of the grating normal.

Another illustration of grating diffraction using wavefronts (surfaces of constant phase) is shown in Fig. 10. The geometrical path difference between light from adjacent grooves is seen to be  $d \sin \alpha + d \sin \beta$ . Since  $\beta < 0$ , the latter term is actually negative. From the principle of interference, only when this

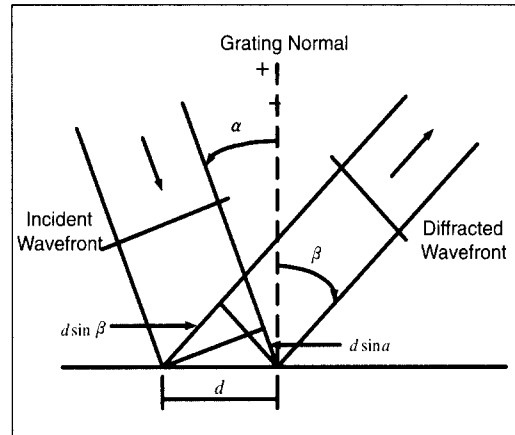


Figure 10. Geometry of diffraction for planar wavefronts

difference equals the wavelength  $\lambda$  of the light, or some integral multiple thereof, will the light from adjacent grooves be in phase leading to constructive interference. At all other angles  $\beta$ , there will be some measure of destructive interference between the wavelets originating from the groove facets.

These relationships are expressed by the grating equation

$$m\lambda = d(\sin \alpha + \sin \beta) \quad (13)$$

which governs angles of diffraction from a grating of groove spacing  $d$ . Here, the integer  $m$  is the diffraction order, or sometimes called spectral order. It is sometimes convenient to write the grating equation as

$$Gm\lambda = \sin \alpha + \sin \beta \quad (14)$$

where  $G = 1/d$  is the groove frequency, groove

density, or pitch, more commonly called “grooves per millimeter.”

It is crucial to note that Eqs. (13) and (14) are valid only when the incident and diffracted rays are perpendicular to the grooves (at the center of the grating). The vast majority of grating systems fail within this category, which is called classical (or in-plane) diffraction. If the incident light beam is not perpendicular to the grooves, the grating equation must be modified as

$$Gm\lambda = \cos \epsilon (\sin \alpha + \sin \beta) \quad (15)$$

where  $\epsilon$  is the angle between the incident light path and the plane perpendicular to the grooves at the grating center. If the incident light lies in this plane,  $\epsilon$  becomes zero and Eq. (15) reduces to Eq. (14). In geometries for which  $\epsilon \neq 0$ , the diffracted spectra lie on a cone rather than in a plane, so such cases are termed conical diffraction.

For a given set of angles  $\alpha$  and  $\beta$ , and groove spacing, the grating equation is valid at more than one wavelength, giving rise to several orders of diffracted radiation. The reinforcement (constructive interference) of diffracted radiation from adjacent grooves occurs when a ray is in phase but retarded by a whole integer. The number of orders produced is limited by the groove spacing and the angle

of incidence, which obviously cannot exceed 90 degrees. At higher orders, efficiency and free spectral range decrease while angular dispersion increases. Order overlap can be compensated by the judicious use of sources, detectors, and filters and is not a major problem in gratings used in low orders. The grooves of a ruled grating have a sawtooth profile with one side longer than the other. The angle  $\theta$  made by a groove's longer side and the plane of the grating is the “blaze angle.” Changing the blaze angle concentrates diffracted radiation to a specified order. The wavelength at which maximum efficiency occurs is the “blaze wavelength.” Holographic gratings are sometimes less efficient than ruled gratings because they cannot be blazed in the classical sense. Their sinusoidal shape can, in some instances, be altered to approach the efficiency of a ruled grating. When the spacing to the wavelength ratio is near one, a sinusoidal grating has virtually the same efficiency as a ruled grating. A holographic grating with 1,800 g/mm can have the same efficiency at 500 nm as a blazed, ruled grating.

Grating efficiency is typically expressed as either “absolute” efficiency or “relative” efficiency. The absolute efficiency of a grating is the percentage of incident monochromatic radiation on a grating that is diffracted into the desired order. This efficiency is determined by both the groove profile (blaze) and the

reflectivity of the grating's coating. In contrast, relative (or groove) efficiency compares the energy diffracted into the desired order with the energy reflected by the plane mirror coated with the same material as the grating.

Angular dispersion of a grating is a function of the angles of incidence and diffraction, the latter of which is dependent upon groove spacing. Angular dispersion can be increased by increasing the angle of incidence or decreasing the distance between successive grooves. A grating with a large angular dispersion can produce good resolution in a compact optical system.

The resolving power of a grating is the product of the diffracted order in which it is used and the number of grooves intercepted by the incident radiation. It can also be expressed in terms of grating width, groove spacing and diffracted angles. Resolving power is a property of the grating and is not, like resolution, dependent on the optical and mechanical characteristics of the system in which it is used. The resolution of an optical system, usually determined by examination of closely spaced absorption or emission lines for adherence to the Rayleigh criteria ( $R = \lambda / \Delta \lambda$ ), depends not only on the grating resolving power but on focal length, slit size,  $f$  number, the optical quality of all components, and

system alignment. The resolution of an optical system is usually much less than the resolving power of the grating.

The surface of standard gratings are coated with aluminum or gold and require extreme care with handling. Handling should be done by the edges only. These relatively soft coatings are vulnerable to fingerprints and numerous aerosols. Scratches or other cosmetic defects do not, unless extreme, usually affect optical performance.

Free spectral range is the wavelength interval that can be obtained in a specified order without spectral interference (overlap) from adjacent orders. As grating spacing decreases, the free spectral range increases. It decreases with higher orders.

Ghosts are defined as spurious spectral lines arising from periodic errors in groove spacing. Interferometrically controlled ruling engines minimize ghosts, while the holographic process eliminates them. On ruled grating, stray light originates from random errors and irregularities of the reflecting surfaces. Holographic gratings generate less stray light because the optical process which transfers the interference pattern to the photoresist is not subject to mechanical irregularities or inconsistencies.

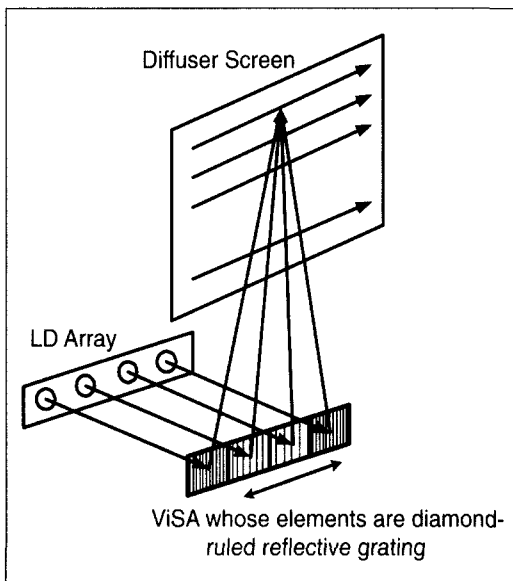


Figure 11 SMV 3-D display system using diamond-ruled reflective grating scanner array

Keeping in mind the characteristics of gratings that have been briefly reviewed in this paper, we can design a new SMV 3-D display system using vibrating reflective grating scanner array as shown in Fig. 11, where diamond-ruled reflective grating array has been attached to a vibrating membrane. The purpose of the grating scanner array is that each of the beams coming out of the laser diodes modulated by the video signal is incident on the corresponding element of the array and scanned over the screen in a parallel manner. As is the case in Section 3, all the beams are directed together to hit one point on the screen by each element of the grating array. It is therefore obvious that every grating has different spatial frequencies to each other.

More than that, each element of the grating array does not have uniform grating spacing over its size. In other words, we have to calculate the different grating spacing for each of the gratings. This may require huge amount of time to finish the calculation. However, once the computation is performed, we can easily copy the original grating by the replication process as described in reference [12, 13].

The replication of a master diffraction grating is four-step process. First, a parting agent is applied to the surface of the master grating; this layer provides poor adherence between the surface of the master grating and the evaporated metallic of the replica grating. A substrate is then cemented with a thin film of low-shrinkage epoxy to the grooved surface of the master grating; this layer is usually 10 to 25 microns in thickness. The epoxy is then cured, resulting in a groove profile that is faithfully replica once the substrate and master are separated.

As an example design of the SMV 3-D display system based on grating scanner array, we will also select the screen that can be used as a practical 3-D display terminal for a computer system. In other words, the size of the screen is 400 mm x 300 mm, just like we did in Sec. 3. Since we want the terminal to be able to support the VGA mode (640 x 480), the resolution of the screen then

becomes  $p = 400/640 = 0.625$  mm. The distance between the grating scanner array and the screen has been set to be  $D = 1$  m. We also assumed the maximum deviation of the vibrating grating to be 1cm. From the parameters that we have selected, we can obtain the minimum beam width  $w$  of the laser diode from the fact that all of the 640 pixels must be mapped into the size of the grating. Since one grating element can deviate 1 cm, the size of the grating element will be  $w = 1 \text{ cm}/640 = 15.6 \mu\text{m}$ , and this is the size of the minimum beam width of the laser diodes. Since the diffraction occurs under the condition that there must be at least 10 grooves within this beam width,  $d$  must be less than  $1.56 \mu\text{m}$ . This number will be used to verify the condition that the computed grating spacing lies in a valid region.

we let laser beam be incident onto the grating with  $\alpha = 0$ , the groove spacing becomes maximum, as long as the computed spacing is less than  $1.56 \mu\text{m}$ . With  $d = 1.56 \mu\text{m}$  and  $\alpha = 0$ , we can find the angles of the first-order diffracted beam as  $\sin^{-1}(0.6328/1.56) = 23.9^\circ$  and second-order diffracted beam as  $\sin^{-1}(2 \times 0.6328/1.56) = 54.2^\circ$ . From this angle, we can calculate the positions of the first-order diffracted beam hitting on the screen as 444 mm and the second-order diffracted beam hitting on the screen as 1,387 mm. This means, as we can see from Fig. 12, that the screen of size 400 mm can fit in the range of 943 mm, and the screen can be as large 943 mm. If we design our SMV 3-D display system which satisfies this condition, there will be no crosstalk between different diffraction orders, and the 3-D image will show up.

Our objective is to compute the grating spacing of the elements of the array. If we use the first order diffracted beam of laser diodes with the wavelength of 632.8 nm, we obtain the groove spacing  $d$ , from Eq. (13), as

$$d = \frac{632.8}{\sin \alpha + \sin \beta} \text{ nm} \quad (13)$$

Equation (13) shows that, if

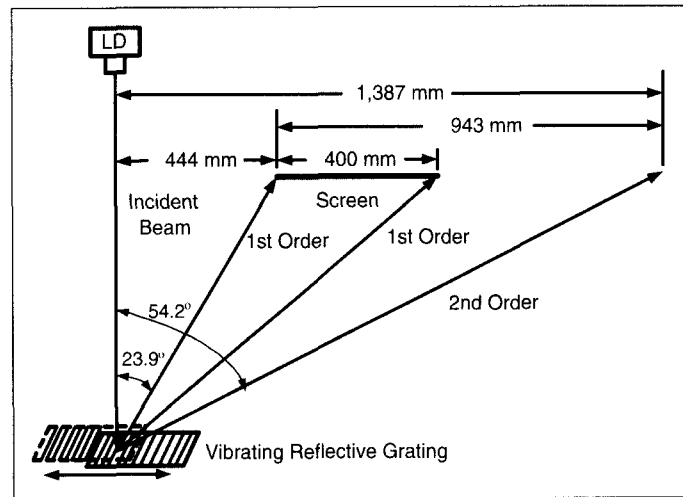


Figure 12 Positions of the 1<sup>st</sup> and 2<sup>nd</sup> order diffracted beam from a grating element for the computation of screen size and incident angle to avoid crosstalk between different orders.

## 6. CONCLUSION

Scanning systems play important roles in 3-D display systems. Especially, polygon mirror and galvanometer scanners have been used for electro-holographic 3-D systems. They have been also used in implementing super multi-view 3-D display system based on focused light array concept proposed by Kajiki. This system, however, requires an imaging lens whose size is as large as the screen size. This becomes impractical when one wants to have large viewing angle with large screens. Moreover, it uses mechanical scanning method, including polygon mirror scanner for horizontal scanning and galvanometer scanner for vertical scanning, which obviously is vulnerable to external physical impact.

In this paper, we proposed a new parallel laser beam scanning method which can be used for super multi-view 3-D display systems based on focused light array concept using a curvature-compensated mirror which is attached to a sinusoidally vibrating membrane. Mathematical analyses for finding the curvature function of the mirror have been presented, and some implementation-related possibilities of the proposed system were addressed.

Based on the mathematical analyses that have been performed in this paper, computer

computations have been done to verify the concept of the proposed system by demonstrating sample designs for the case when the size of the screen is 400 mm x 300 mm with 640 x 480 resolution, and the distance between the curvature-compensated mirror and the screen has been set to be  $D = 100$  mm. With these parameters and different cases of maximum deviation  $A$  and the initial height of the mirror  $r$ , the computer computation results have shown that they are scaled down, and the ratio of the depth of the mirror to the maximum deviation was always 3. This means that we can design CCMS as small as we want, depending upon the types of the vibrating membranes. The beam width of the laser may be a factor that will affect the performance of the system.

Because it is extremely difficult to implement the curvature-compensated mirror scanner array mechanically, we also proposed a different approach, for the sake of easier implementation issue, by adopting diamond-ruled reflective grating array for the parallel scanner. We verified the concept of super multi-view 3-D display system using grating array by presenting the computational results of some fundamental parameters as we did for the curvature-compensated mirror scanner case. We believe that the grating approach will make our system feasible to implement more natural and less eye-fatigue 3-D display system



for the specification of future 3-D TV, providing wider viewing angle with more images that can be presented into viewer's eyes. The proposed system is also robust and

strong to external physical impacts. This will make the 3-D display systems deployed easier and 3-D display industries healthier than ever.

● REFERENCES ●

- [1] T. Okoshi, "Three-Dimensional Displays," Proc. IEEE, Vol. 68, No. 5, May 1980.
- [2] T. Okoshi, Three-Dimensional Imaging Techniques, Academic Press, New York, 1976.
- [3] A. R. L. Travis, "The Display of Three-Dimensional Video Images," Proc. IEEE, Vol. 85, No. 11, November 1997.
- [4] T. Motoki, H. Isono, and I. Yuyama, "Recent Status of 3-Dimensional Television Research," Proc. IEEE, Vol. 83, pp. 1009-1021, July 1995.
- [5] P. St.-Hilaire, S. A. Benton, M. Lucente, M. L. Jepsen, J. Kolln, H. Yoshikawa, and J. Underkoffer, "Electronic Display System for Computational Holography," Proc. SPIE, Vol. 1212, pp. 174-182, 1990.
- [6] J. Y. Son, S. A. Shestak, S. K. Lee, and H. W. Jeon, "Pulsed Laser Holographic Video," Proc. SPIE, Vol. 2652, pp. 24-28, 1996.
- [7] K. Maeno, N. Fukaya, O. Nishikawa, K. Sato, and T. Honda, "Electro-Holographic Display Using 15 Mega Pixels LCD," Proc. SPIE, Vol. 1914, pp. 212-218, 1993.
- [8] J. R. Moore, A. R. L. Travis, S. R. Lang, and O. M. Castle, "Time-Multiplexed Color Autostereoscopic Display," Proc. SPIE, Vol. 2653, pp. 10-19, 1996.
- [9] J. Y. Son, J. S. Kim, and Ho-In Jeon, "Designing a Multi-view 3-D Display System Based on a Spatiotemporal Multiplexing," Journal of Optical Society of Korea - Korean Edition, Vol. 9, pp. 368-372, 1998.
- [10] Y. Kajiki, H. Yoshikawa, and T. Honda, "3-D Display with Focused Light Array," Proc. SPIE, Vol. 2652, pp. 106-116, 1996.
- [11] Ho-In Jeon, et. al., "Super Multi-view 3-D Display System Using Vibrating Scanner Array (VISA)," Journal of Optical Society of Korea, Vol. 4, No. 1, pp. 37 - 42, March 2000
- [12] Christopher Palmer, Diffraction Grating Handbook, 3rd Edition, Richardson Grating Laboratory, New York, 1996.
- [13] <http://www.gratinglab.com>

필자소개



전 호 인

- 1982년 2월 : 경북대학교 전자공학과 졸업
- 1984년 2월 : 서울대학교 대학원 전기공학과 공학석사
- 1993년 2월 : 일본 동경대학 전기공학과 공학박사
- 1984년 1월~1997년 8월 : LG종합기술원 책임연구원
- 1995년 4월~1996년 3월 : 일본 방송통신기구 초빙연구원
- 1997년 9월~현재 : 호서대학교 전기공학부 정보제어공학과
- 주관심 연구분야 : 디지털 신호처리, 디지털 영상통신, 영상처리 및 부호화, Image Sensor 등.

필자소개



**정 낙 희**

- 1993년 2월 : 관동대학교 전자공학과 졸업 공학사
- 1996년 2월 : 연세대학교 산업대학원 전자공학과 졸업 공학석사
- 2001년 8월 : 경원대학교 대학원 전기전자 공학과 공학박사
- 2001년 현재 : 주엽공업고등학교 교사
- 주관심분야 : 3D Display 시스템, 초다시점 3차원 영상 시스템, Focused Light Array



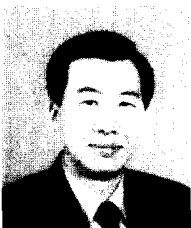
**최 진 산**

- 1994년 2월 : 상보 고등학교 졸업
- 1998년 2월 : 경원대학교 전자공학과 졸업 공학사
- 2001년 2월 : 경원대학교 전기전자 공학과 공학석사학위 취득
- 현재 : 경원대학교 전기전자 공학과 박사학위 재학 중
- 주관심분야 : HomeNetwork 용 미들웨어(UPnP, Jini, VHN), IEEE1394, Bluetooth, 3D Display 시스템



**정 영**

- 1983년 2월 : 연세대학교 공과대학 전자공학과 졸업
- 1997년 2월 : 경원대학원 전자공학과 졸업(공학석사)
- 1997년 3월 ~ 현재 : 경원대학원 박사과정
- 1982년 12월 : 대한전선(주) 정보통신연구소 입사
- 2000년 6월 대한전선(주) 퇴사 (기술담당 이사)
- 2000년 7월 ~ 현재 : 아코텔레콤(주) 대표이사



**허 영**

- 1995년 8월 : 미국 텍사스 주립대학교 전기공학과 졸업(공학박사)
- 1987년 ~ 현재 : 한국전기연구원 영상응용연구 그룹장(책임연구원)
- 1998년 ~ 현재 : 경남대학교, 창원대학교 겸임교수
- 1999년 ~ 현재 : 대한전자공학회 편집위원
- 2001년 ~ 현재 : 한국전기연구원 전자의료기기 종합정보지원센터장
- 주관심 분야 : 영상신호처리, 의료영상 및 산업용 멀티미디어응용기술, 3D영상처리



**김 정 삼**

- 1994년 : 연세대학교 전자공학과 졸업(공학사)
- 1994년 : 체신부 입사
- 1999년 ~ 현재 : 정보통신부 방송위성과